Active Site Residues of *cis*-2,3-Dihydro-2,3-dihydroxybiphenyl Dehydrogenase from *Comamonas testosteroni* Strain B-356[†]

M. Vedadi,[‡] D. Barriault,[§] M. Sylvestre,[§] and J. Powlowski*,[‡]

Department of Chemistry and Biochemistry, Concordia University, Montreal, Quebec, Canada H3G 1M8, and INRS−Santé, Institut National de la Recherche Scientifique, 245 Hymus Boulevard, Pointe-Claire, Québec, Canada H9R 1G6

Received September 24, 1999; Revised Manuscript Received January 18, 2000

ABSTRACT: *cis*-2,3-Dihydro-2,3-dihydroxybiphenyl dehydrogenase (BphB) from *Comamonas testosteroni* strain B-356 is the second enzyme of the biphenyl/polychlorinated biphenyl degradation pathway. Based on the crystal structure of a related BphB, three conserved residues, Ser142, Tyr155, and Lys159, have been suggested to function as a "catalytic triad" as for other members of the short-chain alcohol dehydrogenase/reductase (SDR) family. In this study, substitution of each triad residue was examined in BphB. At pH 9.0, turnover numbers relative to wild-type enzyme were as follows: Y155F, 0.1%; S142A, 1%; and K159A, 10%. Although the Michaelis constants of K159A and S142A for *cis*-2,3-dihydro-2,3-dihydroxybiphenyl increased about 20-fold, relatively little change was observed in the K_m for dinucleotide. The K159A mutant, which showed little dehydrogenase activity at pH 7, was sharply activated by increasing the pH, reaching almost 25% of the activity of the wild-type enzyme at pH 9.8. These three residues are therefore critical for BphB activity, as suggested by the crystal structure and similarity to other SDR family members. In addition, BphB showed a strong preference for NAD^+ over $NADP^+$, with a 260-fold higher specificity constant (k_{cat}/K_m). Evidence is presented that the inefficient use of $NADP^+$ by BphB might partly be due to the presence of an aspartate residue at position 36.

The polychlorinated congeners of biphenyl (PCB's) once had vast industrial application, but now confront society as unusually persistent environmental pollutants. A number of strains of bacteria that can catabolize biphenyl, and cometabolize PCB's, have been isolated from the environment. These include *Comamonas testosteroni* strain B-356 (*1*), *Burkholderia cepacia* strain LB400 (*2*), *Pseudomonas pseudoalcaligenes* strain KF707 (*3*), and *Pseudomonas sp.* strain KKS102 (*4*). The common metabolic pathway for biphenyl has four major steps. A multicomponent biphenyl dioxygenase, comprising a terminal oxygenase (BphAE),[1] ferredoxin (BphF), and ferredoxin reductase (BphG), incorporates two atoms of oxygen into the biphenyl ring. The resulting product, *cis*-2,3-dihydro-2,3-dihydroxybiphenyl, is then dehydrogenated by BphB using NAD^+ (Figure 1), and further metabolized to benzoic acid and 2-oxo-4-pentdienoate by the sequential actions of 2,3-dihydroxybiphenyl dioxygenase (BphC) and a hydrolase (BphD).

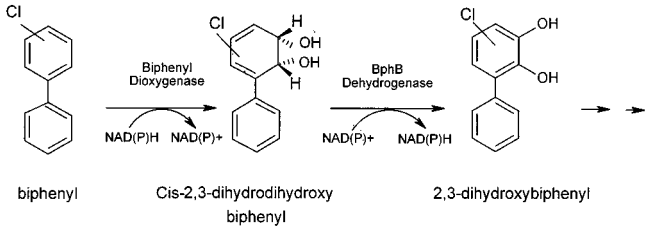

FIGURE 1: First two steps of the metabolic pathway for the bacterial degradation of biphenyl.

BphB from *C. testosteroni* strain B-356 ($BphB_{B\text{-}356}$) is a tetramer with identical subunits of 29.4 kDa. The amino acid sequence of $BphB_{B\text{-}356}$ is about 80% identical to that of BphB from *B. cepacia* strain LB400 ($BphB_{LB400}$), and more distantly related to other *cis*-dihydrodiol dehydrogenases involved in aromatic degradation pathways (*5*−*7*). These dehydrogenases are, in turn, members of a very large family of short-chain alcohol dehydrogenase/reductases (SDR). Although pairwise residue identity within the family is typically only 15−30%, an amino-terminal GXXXGXG nucleotide-binding motif and an active site YXXXK motif are characteristic of all family members (*8*).

Based on sequence similarities and the crystal structure of $BphB_{LB400}$ (*9*), Ser142, Tyr155, and Lys159 of $BphB_{B\text{-}356}$ are candidates to form an active site catalytic triad similar to that described for other members of the SDR family (*8*, *10*−*13*). As was pointed out by Hulsmeyer et al., the triad residues of the active sites of the available SDR structures superimpose with an average RMS deviation of only 0.48 Å (*9*). Therefore, despite the low overall sequence identity, the active site structures of SDR family enzymes

[†] This work was supported by a Strategic grant (STP 0193182) from the Natural Sciences and Engineering Research Council of Canada.

* To whom correspondence should be addressed. Tel: (514) 848-8727; E-mail: powlow@vax2.concordia.ca.

[‡] Concordia University.

[§] INRS−Santé, Institut National de la Recherche Scientifique.

[1] Abbreviations: BphB, *cis*-2,3-dihydro-2,3-dihydroxybiphenyl dehydrogenase; CD, circular dichroism; IPTG, isopropyl β-D-thiogalactopyranoside; MES, 2-(*N*-morpholino)ethanesulfonic acid; NAD^+, β-nicotinamide adenine dinucleotide; $NADP^+$, β-nicotinamide adenine dinucleotide phosphate; $NahB_{G7}$, NahB from *P. putida* G7; SDR, short-chain alcohol dehydrogenase/reductases; SDS−PAGE, sodium dodecyl sulfate−polyacrylamide gel electrophoresis; SYK, triad serine, tyrosine, and lysine residues; wt, wild type.

10.1021/bi992232k CCC: $19.00
Published on Web 04/06/2000

are likely to be quite similar. Nevertheless, since a structure is not available for a BphB/*cis*-2,3-dihydro-2,3-dihydroxybiphenyl complex, the details of the arrangement of the BphB active site are not known with certainty.

Site-directed mutagenesis of the active site SYK triad has been done with a few members of the large and diverse SDR family. Substitution of phenylalanine for the conserved active site tyrosine of three different hydroxysteroid dehydrogenases (*14*−*16*), *Drosophila* alcohol dehydrogenase (*10*), and 15-hydroxyprostaglandin dehydrogenase (*17*) all resulted in enzymes with <0.1% of the wt turnover number. A role for this residue in deprotonation of the alcohol of the substrate has been postulated (*8, 10, 14, 18*). In some cases, replacement of the tyrosine by a readily ionizable residue, cysteine or histidine, yielded active mutants (*10, 16*). It has been suggested that the catalytic triad lysine residue is responsible for deprotonation of the phenolic proton of tyrosine. In general, replacement of the conserved lysine residue by a neutral residue also abolishes enzymatic activity (*10, 14, 15, 17*), although 5% residual activity was observed for K163I *E. coli* 7α-hydroxysteroid dehydrogenase (*16*). By contrast, when the triad lysine was replaced with another basic residue, arginine, mutant enyzmes retained dehydrogenase activity (10−100% of wt k_{cat}) (*10, 15*). Finally, replacement of the triad serine residue by alanine yielded inactive SDR enzymes in three cases (*11*−*13*), but in another case, 20% activity was retained (*16*). Replacement of the serine residue with a threonine resulted in a fully active enzyme, suggesting a role for serine in hydrogen bonding with the substrate/product hydroxyl (*12*).

Another aspect of substrate specificity for *cis*-dihydrodiol dehydrogenases involved in aromatic catabolism concerns the specificity for NAD^+ vs $NADP^+$. In general, it has been reported that these *cis*-dihydrodiol dehydrogenases are inactive when $NADP^+$ is substituted for NAD^+ (*9, 19, 20*). This is an interesting observation since some oxygenases catalyzing *cis*-dihydrodiol formation, such as biphenyl dioxygenase (Figure 1), can oxidize either NADH or NADPH (*2*). The structure of BphB suggests a role for specific residues in determining nucleotide specificity. In the NAD^+−$BphB_{LB400}$ complex, the hydroxyl group of the adenine ribosyl of NAD^+ participates in two hydrogen bonds with Asp36. Enzymes with a negatively charged residue in this position are known to prefer NAD^+ over $NADP^+$ (*21*−*23*). However, in some related dihydrodiol dehydrogenases, such as 1,2-dihydroxy-1,2-dihydronaphthalene dehydrogenase (NahB), Asp36 in $BphB_{LB400}$ is occupied by a neutral residue, Val35 (*5, 6*). Thus, it is of interest to assess the importance of Asp36 in nucleotide discrimination.

In this study, we report for the first time the roles of the SYK triad residues of a *cis*-dihydrodiol dehydrogenase member of the SDR family. The results indicate that these residues are critical for catalytic activity. From a study of the pH dependence of native and mutant enzymes, we obtained evidence for a role of the triad lysine in lowering the pK_a of the active site tyrosine residue. Interestingly, our results indicate that although BphB shows a strong preference for NAD^+, it can indeed use $NADP^+$ as a coenzyme. The importance of Asp36 in determining this preference was investigated by comparison with NahB, where Asp36 is replaced by a neutral residue, Val35.

MATERIALS AND METHODS

Materials. NAD^+ and $NADP^+$ were purchased from Sigma Chemical Co. Restriction enzymes, ligase, DNA purification kits, and IPTG were from Promega. Biphenyl was obtained from Anachemia. All other chemicals were reagent grade or better.

Preparation and Purification of cis-2,3-Dihydro-2,3-dihydroxybiphenyl. cis-2,3-Dihydro-2,3-dihydroxybiphenyl was synthesized using a strain of *E. coli* expressing the biphenyl dioxygenase components of *B. cepacia* strain LB-400. *E. coli* BL21(DE3)*plysS* harboring a T7-polymerase-based plasmid expressing the biphenyl dioxygenase genes (a gift from Dr. Lindsay Eltis, Laval University, Quebec) was grown at 37 °C in Luria−Bertani broth (LB) to OD_{600} of 0.8−0.9: protein expression was induced by addition of IPTG (0.5 mM). Growth was continued for 3 h after which cells were harvested by centrifugation and resuspended in minimal medium. After addition of biphenyl (0.2%), the cell suspension was incubated overnight with agitation. The next day excess biphenyl was removed by filtration through glass wool, and cells were harvested by centrifugation. The product was then purified from the supernatant.

cis-2,3-Dihydro-2,3-dihydroxybiphenyl was purified essentially using the method of Patel and Gibson (*24*). The culture supernatant was extracted using an equal volume of ethyl acetate, which was then dried over anhydrous sodium sulfate. Ethyl acetate was evaporated using a rotary evaporator (30−40 °C), and the residue was dissolved in warm hexane and kept at −20 °C overnight. Crystallized *cis*-2,3-dihydro-2,3-dihydroxybiphenyl was dried under a stream of nitrogen and was kept at −20 °C until use. The presence of *cis*-2,3-dihydro-2,3-dihydroxybiphenyl was monitored during purification by the presence of a peak in the UV spectrum at 306 nm, which is quite distinct from that of biphenyl at 203 nm. About 40−60 mg of *cis*-2,3-dihydro-2,3-dihydroxybiphenyl was typically purified from 1 L of culture. The purity of the final product was greater than 90% as confirmed by HPLC and gas chromatography−mass spectrometry (data not shown) (*1*).

Expression and Purification of $BphB_{B\text{-}356}$. The region encoding BphB (*BphB*) was PCR-amplified from a cloned DNA fragment of *Comamonas testosteroni* strain B-356 in the pQE31 vector (*19*), using *Pwo* polymerase (Boehringer Mannheim). To later subclone the PCR fragment into the pET-3a expression vector (Novagen), *Nde*I and *Bam*HI restriction sites (underlined) were introduced. The primers used for PCR were:

Primer 1:
ATCACCATACGGATCATATGAAGCTGACAGG

Primer 2:
GCTAATTAAGCTTGGATCCAGGTCGACCC

The PCR product was then purified, digested with *Nde*I and *Bam*HI, and ligated to the *Nde*I and *Bam*HI sites in pET-3a. The nucleotide sequence of *bphB* was confirmed in plasmids carrying the insert.

Subsequently, the pET-3a(*bphB*) construct was transformed into *E. coli* BL21(DE3) for expression (*25*). Typically, cells were grown at 37 °C in LB medium (3 L) with

ampicillin (50 μg/mL) to an OD_{600} of 0.8−0.9, at which time IPTG (0.5 mM) was added and growth was continued for 3 h.

BphB was isolated using two purification steps: ammonium sulfate fractionation followed by Fast-Flow DEAE Sepharose chromatography. Cells from 3 L of culture were collected by centrifugation and resuspended in 50 mM sodium phosphate buffer, pH 7 (54 mL), before being lysed by sonication. The lysate was clarified by centrifugation, and ammonium sulfate was added to the supernatant to 40% saturation. After 30 min on ice, precipitated protein was removed by centrifugation, and the pellet was redissolved in 50 mM phosphate buffer, pH 7 (50 mL).

The sample from the previous step was loaded onto a Fast-Flow DEAE Sepharose column (bed volume of ∼60 mL). The column was washed with 50 mM sodium phosphate buffer, pH 7 (200 mL), and eluted in 12 mL fractions with a gradient of sodium phosphate buffer, pH 7 (50−400 mM, 400 mL each). Eluted BphB was detected in fractions 2−16, with fractions 8−10 corresponding to the peak of enzyme activity. Active fractions were combined, concentrated, and stored in 50% glycerol at −20 °C until further use. The final preparation of BphB was pure as judged by SDS−PAGE after staining with Coomassie Blue. Electrospray mass spectrometry was used to determine the molecular weight of BphB and was kindly performed by Elisabeth Cadieux, Concordia University.

Expression and Purification of His-Tagged $BphB_{B\text{-}356}$ and $NahB_{G7}$. His-tagged $NahB_{G7}$ was expressed in *E. coli* and purified by affinity chromatography according to protocols described previously (*19*, *26*). Although $NahB_{G7}$ was stable at −80 °C for a few weeks, diluted $NahB_{G7}$ at 4 °C was quite unstable. For this reason, all experiments were performed as rapidly as possible, each time using a fresh dilution. Expression and purification of his-tagged $BphB_{B\text{-}356}$ have also been described previously (*19*).

Site-Directed Mutagenesis and DNA Sequencing. BphB in the pET-3a vector was mutated using the Quikchange method (Stratagene), following the protocol of the manufacturer. The codons for S142 (TCT), Y155 (TAT), and K159 (AAG) were altered to GCT (alanine), TTT (phenylalanine), and GCG (alanine), respectively. Complementary primers (29−33 bp) were designed with these substitutions, and obtained from BioCorp Inc. (Montreal, Canada). Introduction of the desired mutations was confirmed by sequencing. S142A, Y155F, K159A, S142A/Y155F, and Y155F/K159A mutant BphB enzymes were expressed and purified as described for the wild-type (wt) enzyme.

DNA sequencing was performed at the Sheldon Biotechnology Centre (Montreal, Canada) using a Perkin-Elmer 373A sequencer and ABI sequencing strategy.

Circular Dichroism Spectroscopy. Purified wt $BphB_{B\text{-}356}$ and all mutant enzymes were analyzed in 50 mM sodium phosphate buffer, pH 7, at 25 °C using a JASCO 710 spectropolarimeter. Ellipticity was measured as a function of wavelength from 190 to 260 nm at a protein concentration of 0.2 mg/mL, using a 0.05 cm cell.

Protein Assays. Protein concentration was routinely assayed either by the method of Bradford (*27*), using BSA as a standard, or by measuring the absorption of light at 280 nm. An extinction coefficient of 14 890 M^{-1} cm^{-1} was used to calculate the concentration of purified BphB.

Enzyme Activity Assays. BphB-catalyzed dehydrogenase activity was routinely assayed in 50 mM sodium pyrophosphate buffer, pH 9, at 25 °C. Production of NAD(P)H was monitored by continuously recording the emission at 460 nm after excitation at 340 nm, using a model RF-5000 fluorometer from Shimadzu. The wavelength dispersion was 5 nm for both excitation and emission. Data were analyzed by fitting initial rates to the Lineweaver−Burk equation using linear regression. Values for k_{cat} are reported for the tetramer.

Values of Michaelis constants for $NADP^+$ and NAD^+, using $NahB_{G7}$, $BphB_{B\text{-}356}$, S142A, Y155F, and K159A, were estimated in the presence of saturating *cis*-2,3-dihydro-2,3-dihydroxybiphenyl concentrations (ranging from 0.1 to 0.8 mM, depending upon the mutant enzyme examined). In each case, it was experimentally confirmed that further increases in the concentration of *cis*-2,3-dihydro-2,3-dihydroxybiphenyl did not increase the activity. The Michaelis constants for *cis*-2,3-dihydro-2,3-dihydroxybiphenyl were estimated using saturating concentrations of NAD^+ or $NADP^+$ (2.5 and 20 mM, respectively) and varying the concentration of *cis*-2,3-dihydro-2,3-dihydroxybiphenyl from 0.4 to 1000 μM. Since specific activities were so low, the turnover numbers of the two double mutants were estimated from assays using saturating concentrations of both substrates (0.4−0.8 mM *cis*-2,3-dihydro-2,3-dihydroxybiphenyl and 2 mM NAD^+).

For pH-dependence studies, the activities of wt $BphB_{B\text{-}356}$ and mutant enzymes were assayed at saturating concentrations of *cis*-2,3-dihydro-2,3-dihydroxybiphenyl and $NAD(P)^+$ in either 50 mM sodium phosphate buffer and/or sodium pyrophosphate buffer, and also in a three-component buffer (0.1 M MES, 0.05 M *N*-ethylmorpholine, 0.05 M diethanolamine, and 1 mM EDTA) at various pH values ranging from 6 to 10 (*28*). For wt enzyme, both buffer systems yielded identical results. Hence, phosphate and pyrophosphate buffers were used to construct the pH−rate profile for the mutant proteins. It was experimentally determined that at any given pH, the fixed substrate was present at saturating levels. Rate−pH data were fitted to the appropriate equations using GraFit (version 4.0, Erithacus Software Limited, Middlesex, U.K.).

RESULTS

Expression and Purification of BphB. The gene encoding $BphB_{B\text{-}356}$ was PCR-amplified from a cloned DNA fragment of *C. testosteroni*: *Nde*I and *Bam*HI restriction sites were introduced at the 5′- and 3′-ends of the gene, respectively. The *Nde*I−*Bam*HI fragment was subcloned into the pET-3a vector, and the resulting plasmid was used for expression of $BphB_{B\text{-}356}$ in *E. coli* BL21(DE3).

Recombinant $BphB_{B\text{-}356}$ was very well expressed in *E. coli* (Figure 2, lane 2), allowing the purification of about 50 mg of enzyme/L of cell culture. The purification procedure involved ammonium sulfate precipitation followed by Fast-Flow DEAE-Sepharose chromatography. Precipitation of $BphB_{B\text{-}356}$ from crude extract at 40% saturated ammonium sulfate resulted in a 3.2-fold increase in specific activity. Fast-Flow DEAE-Sepharose chromatography gave a further 2-fold increase in the specific activity of the enzyme (Table 1).

The final preparation was pure, as judged by SDS−PAGE after staining with Coomasie Blue (Figure 2). Electrospray mass spectrometry showed that the molecular mass of

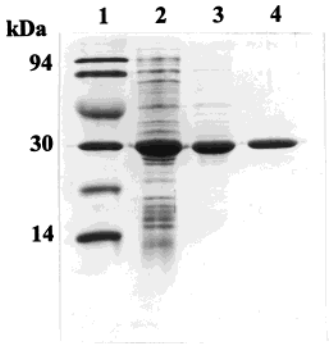

FIGURE 2: Expression and purification of BphB from *C. testosteroni* strain B356. Samples of crude cell lysate, ammonium sulfate precipitate, and pure BphB (lanes 2−4, respectively) were resolved by SDS−PAGE (16%) and stained by Coomassie Blue. Lane 1 contains protein standards.

Table 1: Purification of Recombinant $BphB_{B-356}$

purification step	volume (mL)	total protein (mg)	total activity (U)[a]	specific activity (U/mg)
crude extract	54	1130	3020	2.7
ammonium sulfate precipitation	50	340	2970	8.7
DEAE-Sepharose chromatography	3.9	146	2540	17.4

[a] Represents the conversion of 1 μmol of NAD^+ to NADH per minute at 25 °C and pH 9 in the presence of *cis*-2,3-dihydro-2,3-dihydroxybiphenyl.

purified $BphB_{B-356}$ (29 351 Da) was the same as that expected from the deduced amino acid sequence (data not shown). Purified $BphB_{B-356}$ was stable in 50% glycerol at −20 °C for months. These preparations appeared to be stable over a longer period of time than purified his-tagged $BphB_{B-356}$ (*19*).

Replacement of Putative Catalytic Triad Residues. Based on the high similarity (80% identity) between the amino acid sequences of $BphB_{B-356}$ and $BphB_{LB400}$ (Figure 3) and also the crystal structure of $BphB_{LB400}$ (*9*), members of a putative catalytic triad, Ser142, Tyr155, and Lys159, were replaced by alanine (S142A), phenylalanine (Y155F), or alanine (K159A), respectively. S142A, Y155F, K159A, S142A/Y155F, and Y155F/K159A single and double mutants of $BphB_{B-356}$ were expressed and purified as described for native enzyme. The mutant BphB enzymes were all well expressed and soluble, and exhibited similar behavior during purification (data not shown). To investigate if the amino acid substitutions affected the overall secondary structure of the enzyme, circular dichroic spectra of the mutants were compared to that of wt $BphB_{B-356}$. The spectra for all proteins were very similar, indicating that no gross secondary structural changes occurred as a result of the amino acid substitutions made (data not shown).

Kinetic Properties of Wild-Type and Mutant $BphB_{B-356}$. It has generally been reported that bacterial *cis*-dihydrodiol dehydrogenases from aromatic degradation pathways are inactive with $NADP^+$ as the redox cofactor (*9*, *19*, *20*, *24*). By exploiting a sensitive new fluorometric assay method, we discovered that $BphB_{B-356}$ can also use $NADP^+$ as a coenzyme. $BphB_{B-356}$ activity increased with increasing pH, reaching maximum activity at about pH 9, using either NAD^+ or $NADP^+$ (Figure 4). Kinetic properties of $BphB_{B-356}$ obtained at pH 9 are presented in Table 2. Michaelis constants for NAD^+ and $NADP^+$ were 0.24 and 5.5 mM, respectively. The value of k_{cat} using NAD^+ as a coenzyme (2500 ± 100 min^{-1}) was about 11-fold higher than that obtained using $NADP^+$ (220 ± 35 min^{-1}). As expected, values of k_{cat}/K_m were 260-fold higher for NAD^+ than $NADP^+$, indicating that BphB shows a strong preference for the nonphosphorylated nucleotide. His-tagged $BphB_{B-356}$ was also active with $NADP^+$ and exhibited similar kinetic properties under the assay conditions used in this study (data not shown).

The effects of three amino acid substitutions are summarized in Table 2. Substitution of Tyr155 by phenylalanine (Y155F) decreased k_{cat} 1000-fold, indicating that the hydroxyl group of Tyr155 is critical for enzyme activity. Substitution of Ser142 by alanine decreased k_{cat} by a factor of 100, illustrating the importance of the hydroxyl group of Ser142 in catalysis. Interestingly, the activity of the K159A mutant was only 1 order of magnitude lower than that of the wt enzyme. In addition to affecting turnover numbers, the K159A and S142A substitutions increased the K_m values for *cis*-2,3-dihydro-2,3-dihydroxybiphenyl by 18- and 25-fold, respectively, relative to wt enzyme, which further decreases the efficiency (k_{cat}/K_m) of these mutants. However, little change in the Michaelis constant for $NAD(P)^+$ was observed, demonstrating that these substitutions have relatively small effects on nucleotide binding (Table 2). No Michaelis constants could be reliably estimated for the Y155F mutant because of its very low turnover number.

The presence of residual activity in the Y155F mutant prompted construction of the S142A/Y155F double mutant to test the possibility that S142 could partially replace Y155 as an active site nucleophile. The similar turnover numbers of the two mutant enzymes (Table 2) indicates that this is not the case.

Dependence of Reaction Rates on pH. The rates of the reactions catalyzed by wt and mutant enzymes of $BphB_{B-356}$ increased as the pH was elevated, with the wt enzyme achieving a maximum value between pH 9 and 9.5 (Figure 4). However, the k_{cat} values of wt and mutant forms S142A and Y155F did not show a marked dependence on pH, indicating that for these enzymes there is no *single* ionizable group critical for catalysis that titrates over the experimentally accessible pH range (*29*). Comparison of the relative activities at pH 10, in the presence of NAD^+, indicates that S142A and Y155F catalyze the reaction 2 and 3 orders of magnitude more poorly than wt enzyme. $NADP^+$ can replace NAD^+, but the k_{cat} of the wt enzyme is lower by a factor of about 10. In contrast, K159A is an effective catalyst, showing 25% the turnover number of the wt enzyme at pH 10. Moreover this mutant enzyme shows a pronounced dependence on pH (Figure 4). The $\log(k_{cat})$ increased by a unit for every unit increase in pH, indicating that maximum activity is dependent on the deprotonation of a single ionizable group (*29*). The data for K159A were fitted using nonlinear regression to a single ionization curve: $y = \text{Limit} \cdot 10^{(pH-pK_a)}/[10^{(pH-pK_a)} + 1]$, where Limit is an undefined upper limit and y represents the value of k_{cat} at a particular pH value (GraFit version 4.0). The fit yielded a pK_a value of 9.6 ± 0.02. This pK_a value approaches that of a Tyr side chain unperturbed by environment ($pK_a \approx 10$).

The pH−rate dependence observed for the K159A mutant was abolished in the Y155F/K159A double mutant, as

```
      *          **   * *   *      *  *  *#        *            ***
TOLUD MRLEGEVALVTGGGAGLGRAIVDRYVAEGARVAVLDKSAAGLEALRKLHGDAIVGVEGDV 60
Lb400 MKLKGEAVLITGGASGLGRALVDRFVAEGAKVAVLDKSAERLAELETDHGDNVLGIVGDV 60
Testo MKLTGEVALITGGASGLGRALVDRFVAEGARVAVLDKSAERLRELEVAHGGNAVGVVGDV 60
DoxEC MGNQ-QVVSITGAGSGIGLELVRSFKSAGYYVSALVRNEEQEALLCKEFKDALEIVVGDV 59
NahB7 MGNQ-QVVSITGAGSGIGLELVRSFKLAGYCVSALVRNEEQEALLCNEFKDALEIVVGDV 59

      *                 **  *    *** ***       *       *   *  *** *
TOLUD RSLDSHREAVARCVEAFGKLDCLVGNAGVWDYLTQLVDIPDDLISEAFEEMFEVNVKGYI 120
Lb400 RSLEDQKQAASRCVARFGKIDTLIPNAGIWDYSTALVDLPEESLDAAFDEVFHINVKGYI 120
Testo RSLQDQKRAAERCLAAFGKIDTLIPNAGIWDYSTALADLPEDKIDAAFDDIFHVNVKGYI 120
DoxEC RDHATNEKLIKQTIDRFGHLDCFIANAGIWDYMLS-IEEPWEKISSSFDEIFDINVKSYF 118
NahB7 RDHATNEKLIKQTIDRFGHLDCFIANAGIWDYMLN-IEEPWEKISSSFDEIFDINVKSYF 118

          * ** *    *    * *       ***  * * ***  *     * *  *  ***
TOLUD LAAKAALPALYQSKGSAIFTVSNAGFYPGGGGVLYTAGKHAVIGLIKQLAHEWGPRIRVN 180
Lb400 HAVKACLPALVASRGNVIFTISNAGFYPNGGGPLYTAAKHAIVGLVRELAFELAPYVRVN 180
Testo HAVKACLPALVSSRGSVVFTISNAGFYPNGGGPLYTATKHAVVGLVRQMAFELAPHVRVN 180
DoxEC SGISAALPELKKTNGSVVMTASVSSHAVGGGGSCYIASKHAVLGMVKALAYELAPEVRVN 178
NahB7 SGISAALPELKKTNGSVVMTASVSSHAVGGGGSCYIASKHAVLGMVKALAYELAPEIRVN 178

          **     * *  *           *   ** *   * *     *     *   * *
TOLUD GIAPGGILGSDLRGLKSLDLQDKSISTFP-LDDMLKSVLPTGRAATAEEYAGAYVFFATR 239
Lb400 GVGSGGIN-SDLRGPSSLGMGSKAISTVP-LADMLKSVLPIGRMPEVEEYTGAYVFFATR 238
Testo GVAPGGMN-TDLRGPSSLGLSEQSISSVP-LADMLKSVLPIGRMPALEEYTGAYVFFATR 238
DoxEC AVSPGGTV-TSLCGSASAGFDKMHMKDMPGIDDMIKGLTPLGFAAKPEDVVAPYLLLASR 237
NahB7 AVSPGGTV-TSLCGPASAGFDKMHMKDMPGIDDMIKGLTPLGFAAKPEDVVAPYLLLASR 237

           **     ***
TOLUD GDTVPLTGSVLNFDGGMGVRGLFEASLGAQLDKHFG------- 275
Lb400 GDAAPATGALLNYDGGLGVRGFFSGAGGNDLLEQLNIHP---- 277
Testo GDSLPATGALLNYDGGMGVRGFLTAAGGADLPEKLNINREGQE 281
DoxEC KQGKFITGTVISIDGGMALGRK---------------------- 259
NahB7 KQGKFITGTVISIDGGMALGRK---------------------- 259
```

FIGURE 3: Amino acid sequence comparison of BphB from *Pseudomonas sp*. strain LB400 (LB400) (*30*) with *cis*-toluene dihydrodiol dehydrogenase from *P. putida* (TOLUD) (*7*), BphB from *C. testosteroni* strain B-356 (Testo) (*19*), 1,2-dihydroxy-1,2-dihydronaphthalene dehydrogenase from *Pseudomonas sp.* strain C18 (DoxEC) (*6*), and 1,2-dihydroxy-1,2-dihydronaphthalene dehydrogenase from *P. putida* G7 (NahB7) (*5*). All conserved residues including glycines at positions 12, 16, and 18 are indicated by (*) while aspartate 36 (LB400 numbering) has been marked by #.

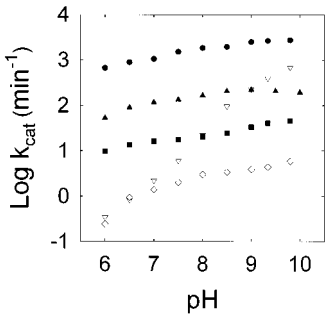

FIGURE 4: Variation with pH of log k_{cat} for the reaction catalyzed by wt BphB assayed in the presence of NAD^+ (●) or $NADP^+$ (▲), and of S142A (■), Y155F (◇), and K159A (▽) mutants assayed in the presence of NAD^+. The assay conditions are described under Materials and Methods.

indicated by the similarity of estimated k_{cat} values at pH 9 (0.6 min^{-1}, Table 2) and pH 7 (0.2 min^{-1}). This result confirms that the titrating group in the K159A mutant (Figure 4) is Y155.

Structural Basis for the Nucleotide Specificity of BphB$_{B\text{-}356}$. $BphB_{B\text{-}356}$ exhibited a strong preference for NAD^+ over $NADP^+$, as do other aromatic *cis*-dihydrodiol dehydrogenases. One of the structural features that discriminates against $NADP^+$ is likely to be the presence of a negatively charged residue at position 36 of $BphB_{B\text{-}356}$ (Asp36), which repels the negatively charged phosphate of $NADP^+$. To test this hypothesis, asparagine and valine residues were substituted at position 36 of BphB. Unfortunately, the resulting mutants (D36N and D36V) were found in inclusion bodies. An alternative approach using a related *cis*-dihydrodiol dehydrogenase was therefore used, and is outlined below.

NahB from *P. putida* G7 has been shown previously to catalyze the same range of reactions as $BphB_{B\text{-}356}$ (*5*). Residues involved in nucleotide binding in BphB are also conserved in $NahB_{G7}$, which, significantly, contains Val35 instead of the negatively charged Asp36 found in BphB (Figure 3). The kinetics of $NahB_{G7}$ were examined using a his-tagged form of the enzyme. Values of k_{cat}/K_m show that $NahB_{G7}$ catalyzes the reaction in the presence of $NADP^+$ 7.5 times more effectively than $BphB_{B\text{-}356}$. However, NahB still prefers NAD^+ as a cofactor, since k_{cat}/K_m is 60-fold higher for NAD^+ compared to $NADP^+$ (Table 2).

DISCUSSION

Amino acid sequence comparisons of $BphB_{B\text{-}356}$ (*19*) with $BphB_{LB400}$ (*30*), *cis*-toluene dihydrodiol dehydrogenase from *P. putida* (*7*), DoxE from *Pseudomonas sp.* C18 (*6*), and $NahB_{G7}$ from *P. putida* G7 (*5*) show that although these dihydrodiol dehydrogenases belong to different aromatic degradation pathways, 72 residues are absolutely conserved among them (Figure 3). Based on the crystal structure of $BphB_{LB400}$, whose amino acid sequence is 80% identical to that of $BphB_{B\text{-}356}$, conserved residues Ser142, Tyr155, and

Table 2: Kinetic Properties of $BphB_{B-356}$, $BphB_{B-356}$ Mutants, and $NahB_{G7}$ at pH 9 and 25 °C

enzyme	coenzyme	K_m 2,3DDBPH[a] (μM)	K_m NAD(P)$^+$ (mM)	k_{cat} (min^{-1})	$k_{cat}/K_{m,NAD(P)^+}$ ($\times 10^{-3}\,min^{-1}mM^{-1}$)
BphB	NAD^+	3.1 ± 0.5	0.24 ± 0.01	2500 ± 100	10.4
NahB		16.8 ± 2.7	0.14 ± 0.03	2500 ± 320	17.8
K159A		55.7 ± 7.1	0.11 ± 0.01	230 ± 40	2.1
S142A		78 ± 36	0.05 ± 0.004	33 ± 10	0.7
Y155F		ND[b]	ND	3.1 ± 0.7	−
S142A/Y155F		ND	ND	2.6 ± 0.2[c]	−
Y155F/K159A		ND	ND	0.6 ± 0.2[c]	−
BphB	$NADP^+$	2.5 ± 0.6	5.5 ± 0.2	220 ± 35	0.04
NahB		27.5 ± 1	3.3 ± 1.8	1030 ± 200	0.3

[a] *cis*-2,3-Dihydro-2,3-dihydroxybiphenyl. [b] ND, not determined. [c] Average of 4 determinations in the presence of saturating concentrations of both substrates.

Lys159 have been suggested to form a catalytic triad in the active site (*9*). Roles for conserved triad residues have been investigated in more distantly related members of the SDR family, but to our knowledge never in a member of the *cis*-dihydrodiol dehydrogenase branch. In the present study, $BphB_{B-356}$ mutants, in which each of these residues were replaced, have been generated and studied.

Replacement of Tyr155 by phenylalanine in the active site inactivated $BphB_{B-356}$ (Table 2), indicating that the hydroxyl side chain of Tyr155 is involved in the catalytic mechanism of the enzyme. Similar results have been reported previously for other members of the SDR family (*8, 10*). Results of the pH−rate studies reported here suggest that Lys159 may be involved in deprotonating the active site nucleophile, Tyr155. Lys159 is in close contact with Tyr155 in the active site of $BphB_{LB400}$ (*9*) and hence could perturb the pK_a of the Tyr residue downward so that the pH optimum of the wt enzyme is about 9. This occurs as the deprotonated form of Lys159 removes a proton from Tyr155's hydroxyl group. In the absence of Lys159, the pK_a of Tyr155 is no longer perturbed downward but rather remains at about 10. As shown in Figure 4, replacing Lys159 in $BphB_{B-356}$ by alanine resulted in a marked shift in the pH−rate profile to alkaline pH. The mutant enzyme is only active at high pH values, where base rather than a lysine residue directly deprotonates the Tyr155 hydroxyl group. Furthermore, the insensitivity of wt enzyme activity to pH (Figure 4) indicates that deprotonation of the tyrosine residue is not rate-limiting.

The position of the side chain of Lys159 in the active site of the enzyme appears very critical. The substitution by Ile of Lys156 in *Drosophila* alcohol dehydrogenase, where it is part of the triad in the active site, inactivated the enzyme while substitution by arginine decreased the activity to 2.2% of the wt (*10*). Introduction of a large side chain in this position may involve unfavorable steric interactions. Complete elimination of the side chain of Lys159 in K159A, however, yielded an active mutant of $BphB_{B-356}$, allowing characterization of the role of the side chain of Lys159 using pH studies.

Ser142 has been proposed to hydrogen bond with a hydroxyl group of *cis*-2,3-dihydro-2,3-dihydroxybiphenyl in the active site of $BphB_{LB400}$ (*9*). In the present study, replacing Ser142 with an Ala in $BphB_{B-356}$ yielded an enzyme that shows 1% of the k_{cat} for the wild-type enzyme. Although this substitution in some members of the SDR family caused complete inactivation (*11*−*13*), replacement with threonine resulted in an active mutant of 3α/17α-hydroxysteroid dehydrogenase (*12*). Such a result is consistent with a role for this residue in hydrogen bonding with the substrate. For the S142A mutant of $BphB_{B-356}$, the Michaelis constants for dinucleotide actually decreased by a factor of 4, but the K_m for *cis*-2,3-dihydro-2,3-dihydroxybiphenyl rose 26-fold (Table 2), indicating that Ser142 interacts with and stabilizes substrate binding, likely by hydrogen bonding. Taken together, our results clearly indicate that Ser142, Tyr155, and Lys159 are critical residues in the active site of $BphB_{B-356}$ and support previous conclusions based on the crystal structure of $BphB_{LB400}$ (*9*) and on studies of other members of the SDR family (*10*−*13*).

The nucleotide binding site of $BphB_{LB400}$ (*9*), as in other SDR family members, is located at the amino terminal of the enzyme and comprises the putative glycine-rich fingerprint ($G_{12}XXXGXG_{18}$), which interacts with the pyrophosphate of the bound dinucleotide (*22, 23, 31, 32*). Amino acid sequence alignment (Figure 3) shows that Gly12, Gly16, and Gly18 are among 19 conserved glycine residues. In addition, most of the other residues involved in hydrogen bonding with the dinucleotide at the active site of $BphB_{LB400}$ are conserved in $BphB_{B-356}$, DoxE, and $NahB_{G7}$ (including Ser15, Asp59, and Tyr119). A negatively charged residue in $BphB_{LB400}$, Asp36, hydrogen bonds to the 2′-hydroxyl of the adenine ribose of NAD^+ (*9*). Dehydrogenases possessing an acidic residue at this position are known to prefer NAD^+ over $NADP^+$, since a phosphate group on the 2′-hydroxyl of the ribose ring is repelled by the negatively charged side chain (*21*−*23, 33*). While an acidic residue is conserved at position 36 in $BphB_{B-356}$ and *cis*-toluene dihydrodiol dehydrogenase from *P. putida*, it is replaced by a valine in $NahB_{G7}$ and DoxE (Figure 3). Unfortunately, we were unable to investigate the importance of Asp36 in $BphB_{B-356}$ directly since mutants were insoluble. However the related enzyme, $NahB_{G7}$, was found to use $NADP^+$ more efficiently (7.5-fold higher k_{cat}/K_m) than BphB, which may correlate with the absence of a residue equivalent to Asp36. However, since $NahB_{G7}$ exhibits a Michaelis constant for NAD^+ very close to that found for $BphB_{B-356}$, it raises the question of why the absence of a negatively charged residue (Asp36), which is supposed to hydrogen bond with the 2′-hydroxyl of adenine ribose, has such a small effect on the affinity of the enzyme for NAD^+.

Substitution of the negatively charged residue which hydrogen bonds with the 2′-hydroxyl of the adenine ribose

of NAD^+ is known to affect the Michaelis constant for NAD^+ of some enzymes (*33*, *34*), but not others (*35*). As noted above, the absence of a negatively charged residue in $NahB_{G7}$ also affected the K_m relatively little. The crystal structure of $BphB_{LB400}$ reveals why the absence of the structurally equivalent aspartate may have relatively little effect on the nucleotide specificity of the aromatic *cis*-dihydrodiol dehydrogenases. Unlike dehydrogenases of the SDR family that only form one or two hydrogen bonds with the pyrophosphate of the dinucleotide cofactor (*36*, *37*), six hydrogen bonds connect the pyrophosphate to BphB (*9*). Ser15 is one of the residues that interact with NAD^+, and this is conserved in the amino acid sequence of $NahB_{G7}$ (Figure 3). Additional contacts to the nucleotide are through residues 189−191. Leu191 is also conserved in $NahB_{G7}$, but Ser189 is replaced by threonine, which is also capable of hydrogen bonding. Asp59 interacts with the adenine ring of NAD^+, the only interaction of this type between the protein and adenine ring of the nucleotide. This residue is also conserved in the $NahB_{G7}$ sequence (Figure 3). Such a close similarity in primary sequence in the nucleotide binding region, as well as very strong interaction through six hydrogen bonds between the protein and NAD^+, may be the reason the lack of two extra hydrogen bonds, between Asp36 and NAD^+, fails to significantly perturb the affinity of the enzyme for NAD^+.

This study has provided important biochemical evidence for the functional significance of several active site residues of a *cis*-dihydrodiol dehydrogenase involved in bacterial degradation of polychlorinated biphenyls. This information provides the basic groundwork for rational manipulation of the active site of BphB to accommodate a broader range of substrates. These include chloro-substituted *cis*-dihydrodiols and 3,4-*cis*-dihydrodiols that are generated from some PCB congeners and are relatively poor substrates for BphB (*5*, *38*), limiting the versatility of the biphenyl degradation pathway.

ACKNOWLEDGMENT

We are indebted to Drs. Joanne Turnbull and Lena Sahlman for critical insight and suggestions on the manuscript.

REFERENCES

1. Hurtubise, Y., Barriault, D., Powlowski, J., and Sylvestre, M. (1995) *J. Bacteriol. 177*, 6610−6618.
2. Haddock, J. D., Nadim, L. M., and Gibson, D. T. (1993) *J. Bacteriol. 175*, 395−400.
3. Taira, K., Hirose, J., Hayashida, S., and Furukawa, K. (1992) *J. Biol. Chem. 267*, 4844−4853.
4. Fukuda, M., Yasukochi, Y., Kikuchi, Y., Nagata, Y., Kimbara, K., Horiuchi, H., Takagi, M., and Yano, K. (1994) *Biochem. Biophys. Res. Commun. 202*, 850−856.
5. Barriault, D., Vedadi, M., Powlowski, J., and Sylvestre, M. (1999) *Biochem. Biophys. Res. Commun. 260*, 181−187.
6. Denome, S. A., Stanley, D. C., Olson, E. S., and Young, K. D. (1993) *J. Bacteriol. 175*, 6890−6901.
7. Zylstra, G. J., and Gibson, D. T. (1989) *J. Biol. Chem. 264*, 14940−14946.
8. Jörnvall, H., Persson, B., Krook, M., Atrian, S., Gonzalez-Duarte, R., Jeffery, J., and Ghosh, D. (1995) *Biochemistry 34*, 6003−6013.
9. Hulsmeyer, M., Hecht, H. J., Niefind, K., Hofer, B., Eltis, L. D., Timmis, K. N., and Schomburg, D.(1998) *Protein Sci. 7*, 1286−1293.
10. Chen, Z., Jiang, J. C., Lin, Z. G., Lee, W. R., Baker, M. E., and Chang, S. H. (1993) *Biochemistry 32*, 3342−3346.
11. Ensor, C. M., and Tai, H. H. (1996) *Biochem. Biophys. Res. Commun. 220*, 330−333.
12. Oppermann, U. C., Filling, C., Berndt, K. D., Persson, B., Benach, J., Ladenstein, R., and Jörnvall, H. (1997) *Biochemistry 36*, 34−40.
13. Cols, N., Atrian, S., Benach, J., Ladenstein, R., and Gonzalez-Duarte, R. (1997) *FEBS Lett. 413*, 191−193.
14. Obeid, J., and White, P. C. (1992) *Biochem. Biophys. Res. Commun. 188*, 222−227.
15. Nakajin, S., Takase, N., Ohno, S., Toyoshima, S., and Baker, M. E. (1998) *Biochem. J. 334*, 553−557.
16. Tanabe, T., Tanaka, N., Uchikawa, K., Kabashima, T., Ito, K., Nonaka, T., Mitsui, Y., Tsuru, M., and Yoshimoto, T. (1998) *J. Biochem. (Tokyo) 124*, 634−641.
17. Ensor, C. M., and Tai, H. H. (1994) *Biochim. Biophys. Acta 1208*, 151−156.
18. Albalat, R., Gonzalez-Duarte, R., and Atrian, S. (1992) *FEBS Lett. 308*, 235−239.
19. Sylvestre, M., Hurtubise, Y., Barriault, D., Bergeron, J., and Ahmad, D. (1996) *Appl. Environ. Microbiol. 62*, 2710−2715.
20. Khan, A. A., Wang, R. F., Nawaz, M. S., and Cerniglia, C. E. (1997) *FEMS Microbiol. Lett. 154*, 317−324.
21. Baker, P. J., Britton, K. L., Rice, D. W., Rob, A., and Stillman, T. J. (1992) *J. Mol. Biol. 228*, 662−671.
22. Wierenga, R. K., and Hol, W. G. (1983) *Nature 302*, 842−844.
23. Wierenga, R. K., Terpstra, P., and Hol, W. G. (1986) *J. Mol. Biol. 187*, 101−107.
24. Patel, T. R., and Gibson, D. T. (1974) *J. Bacteriol. 119*, 879−888.
25. Studier, F. W., Rosenberg, A. H., Dunn, J. J., and Dubendorff, J. W. (1990) *Methods Enzymol. 185*, 60−89.
26. Barriault, D., Durand, J., Maaroufi, H., Eltis, L. D., and Sylvestre, M. (1998) *Appl. Environ. Microbiol. 64*, 4637−4642.
27. Bradford, M. M. (1976) *Anal. Biochem. 72*, 248−254.
28. Ellis, K. J., and Morrison, J. F. (1982) *Methods Enzymol. 87*, 405−426.
29. Dixon, M., and Webb, E. C. (1964) *Enzymes*, 2nd ed., Academic Press, New York.
30. Hofer, B., Eltis, L. D., Dowling, D. N., and Timmis, K. N. (1993) *Gene 130*, 47−55.
31. Rossman, M. G., Moras, D., and Olsen K. W. (1974) *Nature 250*, 194−199.
32. Rossman, M. G., Liljas, A., Branden, C. I., and Banaszal, C. J. (1975) *Enzymes* (3rd Ed.) *11*, 61−102.
33. Fan, F., Lorenzen, J. A., and Plapp, B. V. (1991) *Biochemistry 30*, 6397−6401.
34. Metzger, M. H., and Hollenberg, C. P. (1995) *Eur. J. Biochem. 228*, 50−54.
35. Chen, Z., Lee, W. R., and Chang, S. H. (1991 *Eur. J. Biochem. 202*, 263−267.
36. Tanaka, N., Nonaka, T., Nakanishi, M., Deyashiki, Y., Hara, A., and Mitsui, Y. (1996) *Structure 4*, 33−45.
37. Tanaka, N., Nonaka, T., Tanabe, T., Yoshimoto, T., Tsuru, D., and Mitsui, Y. (1996) *Biochemistry 35*, 7715−7730.
38. Haddock, J. D., and Gibson, D. T. (1995) *J. Bacteriol. 177*, 20−26.

BI992232K